

# Investigation of the emission radii of kHz QPOs for the accreting millisecond X-Ray pulsars, Atoll and Z sources

D. H. Wang<sup>1,2,3\*</sup>, L. Chen<sup>2</sup>, C. M. Zhang<sup>3</sup>, Y. J. Lei<sup>3</sup>, J. L. Qu<sup>4</sup>, L. M. Song<sup>4</sup>

<sup>1</sup>*School of Physics and Electronic Science, Guizhou Normal University, Guiyang, 550001, China*

<sup>2</sup>*Astronomy Department, Beijing Normal University, Beijing, 100875, China*

<sup>3</sup>*National Astronomical Observatories, Chinese Academy of Sciences, Beijing, 100012, China*

<sup>4</sup>*Institute of High Energy Physics, Chinese Academy of Sciences, Beijing, 100049, China*

Released 2002 Xxxxx XX

## ABSTRACT

We infer the emission positions of twin kilohertz quasi-periodic oscillations (kHz QPOs) in neutron star low mass X-ray binaries (NS-LMXBs) based on the Alfvén wave oscillation model (AWOM). For most sources, the emission radii of kHz QPOs cluster around a region of 16 – 19 km with the assumed NS radii of 15 km. Cir X-1 has the larger emission radii of 23 ~ 38 km than those of the other sources, which may be ascribed to its large magnetosphere-disk radius or strong NS surface magnetic field. SAX J1808.4-3658 is also a particular source with the relative large emission radii of kHz QPOs of 20 ~ 23 km, which may be due to its large inferred NS radius of 18 ~ 19 km. The emission radii of kHz QPOs for all the sources are larger than the NS radii, and the possible explanations of which are presented. The similarity of the emission radii of kHz QPOs (~ 16 – 19 km) for both the low/high luminosity Atoll/Z sources is found, which indicates that both sources share the similar magnetosphere-disk radii.

**Key words:** stars:neutron-binaries: close-X-rays: binaries-accretion: accretion disks

## 1 INTRODUCTION

The launch of the Rossi X-ray Timing Explorer (RXTE) has led to the discovery of kilohertz quasi-periodic oscillations (kHz QPOs) in neutron star (NS) low mass X-ray binaries (LMXBs) (van der Klis et al. 1996; Strohmayer et al. 1996). These high-frequency QPOs usually appear in pairs (upper  $\nu_2$  and lower  $\nu_1$ ) at frequencies from a few hundred Hz to more than 1 kHz, as shown in Atoll sources, Z sources (see Hasinger & van der Klis 1989 for the definition of Atoll and Z sources) and the accreting millisecond X-Ray pulsars (AMXPs) (see van der Klis 2006 for a review). It is suggested that kHz QPOs might be used to test the General Relativity in a strong gravitational field regime (Miller et al. 1998; Stella & Vietri 1999), and help to constrain the NS *Mass – Radius* relation (Miller et al. 1998).

The frequencies of the kHz QPOs are strongly correlated with other timing and spectral features, such as the photon indexes of the power-law component of the energy spectrum (Kaaret et al. 1998), the noise features (Ford & van der Klis 1998c), the positions in the X-ray

color-color diagram (e.g., Wijnands et al. 1997b), the X-ray luminosities (Méndez et al. 1999b; Ford et al. 2000), the low frequency QPOs (Psaltis et al. 1999; Belloni et al. 2002), where the high-/low-frequency correlation is similar to those in black hole candidates and white dwarf cataclysmic variables (e.g. Psaltis et al. 1999; Belloni et al. 2002; Warner & Woudt 2002; Mauche 2002). Besides, the quality factors and *rms* amplitudes of the kHz QPOs can vary as a function of the QPO frequencies (e.g., Méndez et al. 2001; Barret et al. 2005b).

There is currently no consensus as to the origin of these QPOs. Some interpretations, such as the beat frequency model by Miller et al. (1998); Lamb & Miller (2001) and the resonance model by Kluźniak & Abramowicz (2001); Abramowicz et al. (2003a,b), encounter difficulties when interpreting the following observational characteristics of the kHz QPOs (Belloni et al. 2005, 2007). While the relativistic precession model (Stella & Vietri 1999; Stella et al. 1999) fits the  $\Delta\nu$  vs.  $\nu_2$  relation to the kHz QPO data quite well. However, it requires the NS mass of 2 solar mass ( $M_\odot$ ) (van der Klis 2006), which is relative higher than the actual measurement results (Wang et al. 2013).

The Alfvén wave oscillation model (AWOM) by Zhang (2004) makes a good description of the kHz QPO data

\* huazai05105220@163.com

(Belloni et al. 2007). The model predicts the relative emission positions of the kHz QPOs ( $X \equiv R/r$ , the ratio between the NS radius and the kHz QPO emission radius), which can help to infer the emission radii of kHz QPOs, then further infer the magnetosphere-accretion disk structure and evaluate the possibility of the kHz QPO mechanism.

In this paper we analyze the emission positions of kHz QPOs based on AWOM: In § 2, we introduce the AWOM and show the kHz QPO data used in the paper. In § 3 we infer the emission radii of kHz QPOs and analyze the results for the particular sources. In § 4 we make discussions and conclusions.

## 2 THE MODEL AND DATA

### 2.1 The magnetosphere-disk radius

It is thought that kHz QPOs reflect the motion of matter in orbit at some preferred radius in the accretion disk around the neutron star in LMXBs (Miller et al. 1998; Stella & Vietri 1999; Osherovich & Titarchuk 1999; Lamb & Miller 2001; Zhang 2004). And in order to consider the interaction between the accretion flow and the magnetic field of NS, we introduce the magnetosphere-disk radius  $r_m$ , where the kinetic energy of the free-falling gas becomes comparable to the magnetic energy of the NS magnetosphere (Shapiro & Teukolsky 1983):

$$r_m = \xi r_A = \xi \left( \frac{\mu^4}{2GM\dot{M}} \right)^{1/7} \quad (1)$$

where  $\xi$  is a constant factor that is usually taken as 0.5 (Ghosh & Lamb 1979),  $r_A$  is the Alfvén radius,  $\mu$  is the magnetic moment of NS,  $G$  is the gravitational constant,  $M$  is the NS mass and  $\dot{M}$  is the accretion rate at the inner disk boundary.

We assume the NS magnetic field to be dipolar:

$$B(r) = B_s \left( \frac{R}{r} \right)^3 \quad (2)$$

where  $B_s$  is the NS surface dipole magnetic field strength,  $R$  is the NS radius and  $r$  is the radial distance refer to the center of the NS, and it can be seen that the magnetic field strength decreases with  $r^3$ . Then we adopt the accreting NS mass  $M$  of  $1.6 M_\odot$  based on its standard value of  $1.4 M_\odot$  (the NS mass in LMXBs is averagely increased by about  $0.2 M_\odot$  on account of the accretion, see Zhang et al. 2011) and assume the NS radius  $R$  of 15 km, then the magnetosphere-disk radius can be written as:

$$r_m \approx 7(\text{km}) \left( \frac{B_s}{10^{18} \text{G}} \right)^{4/7} \left( \frac{\dot{M}}{10^{18} \text{g s}^{-1}} \right)^{-2/7}. \quad (3)$$

### 2.2 AWOM

In AWOM, the upper kHz QPO frequency  $\nu_2$  is assumed as the Keplerian orbital frequency  $\nu_K$  of the accretion flow at the preferred radius  $r$  (Zhang 2004):

$$\nu_2 = \nu_K = \sqrt{\frac{GM}{4\pi^2 r^3}} \quad (4)$$

while the lower kHz QPO frequency  $\nu_1$  is interpreted as the MHD Alfvén wave oscillation frequency there. The model

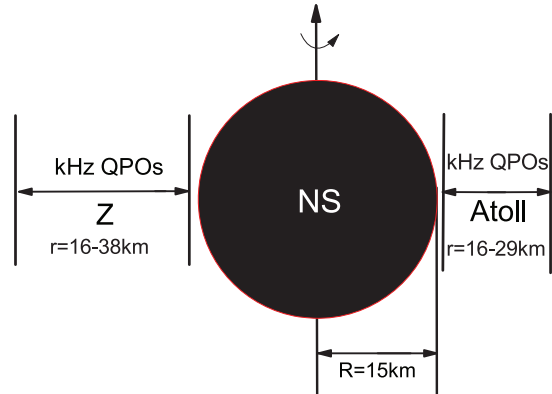


**Figure 1.** The schematic diagram of the emission radii of kHz QPOs for Atoll and Z sources.  $R$  is the NS radius that is assumed to be 15 km, and  $r$  is the radial emission radius of kHz QPOs with the range of 16 – 29 km and 16 – 38 km for Atoll and Z sources, respectively (see Table 1 and Table 2 for the details).

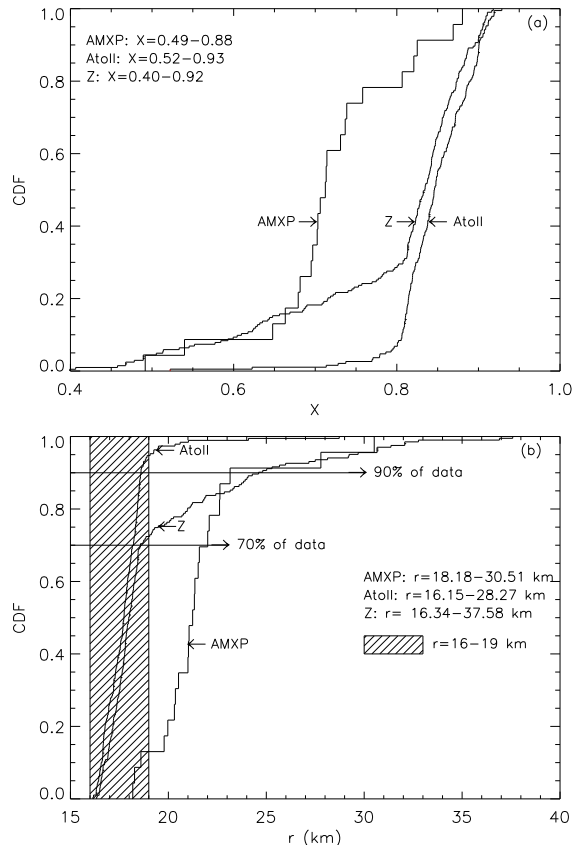


**Figure 2.** (a) The CDF curves of the position parameter  $X$  values. The abscissa and ordinate represent the  $X$  values and the CDF values respectively, and the arrows indicate the curves for AMXPs ( $X = 0.49 - 0.88$ ), Atoll ( $X = 0.52 - 0.93$ ) and Z ( $X = 0.40 - 0.92$ ) sources. (b) Same as (a), but for the emission radius  $r$  of kHz QPOs (the corresponding ranges of  $r$  are 18.18 – 30.51 km, 16.15 – 28.27 km and 16.34 – 37.58 km for AMXPs, Atoll and Z sources respectively), and the shaded area shows the radius range of 16-19 km, which contains most of the data of Atoll sources ( $> 90\%$ ) and Z sources ( $> 70\%$ ) (see Table 1 and Table 2 for the details).

**Table 1.** The frequency ranges and the emission radii of kHz QPOs.

Source (25)	$\nu_1$ (Hz)	$\nu_2$ (Hz)	$X$ ( $\equiv R/r$ )	$r^\dagger$ (km)	References
AMXP (2)					
SAX J1808.4-3658	499 ~ 504	685 ~ 694	0.87 ~ 0.88	–	1
XTE J1807.4-294	106 ~ 370	337 ~ 587	0.49 ~ 0.83	18.18 ~ 30.51	2
Atoll (15)					
4U 0614+09	153 ~ 843	449 ~ 1162	0.52 ~ 0.88	17.02 ~ 28.72	3
4U 1608-52	473 ~ 867	799 ~ 1104	0.77 ~ 0.92	16.32 ~ 19.49	4
4U 1636-53	529 ~ 979	823 ~ 1228	0.81 ~ 0.93	16.15 ~ 18.50	5
4U 1702-43	722	1055	0.84	17.78	6
4U 1705-44	776	1074	0.87	17.21	7
4U 1728-34	308 ~ 894	582 ~ 1183	0.71 ~ 0.90	16.69 ~ 21.02	8
4U 1735-44	641 ~ 900	982 ~ 1149	0.82 ~ 0.91	16.44 ~ 18.32	9
4U 1820-30	764 ~ 796	1055 ~ 1072	0.86 ~ 0.89	–	10
4U 1915-05	224 ~ 707	514 ~ 1055	0.62 ~ 0.83	18.02 ~ 24.09	11
Aql X-1	795 ~ 803	1074 ~ 1083	0.88	16.95 ~ 16.96	12
IGR J17191-2821	681 ~ 870	1037 ~ 1185	0.82 ~ 0.88	17.05 ~ 18.31	13
KS 1731-260	898	1159 ~ 1183	0.90 ~ 0.91	16.53 ~ 16.71	14
SAX J1750.8-2900	936	1253	0.89	16.88	15
XTE J1701-407	745	1150	0.82	18.40	16
XTE J2123-058	847 ~ 871	1102 ~ 1141	0.89 ~ 0.90	16.61 ~ 16.77	17
Z (8)					
Cir X-1	56 ~ 226	229 ~ 505	0.40 ~ 0.64	23.36 ~ 37.58	18
Cyg X-2	516	862	0.77	–	19
GX 5-1	156 ~ 662	478 ~ 888	0.51 ~ 0.89	16.90 ~ 29.69	20
GX 17+2	475 ~ 830	759 ~ 1079	0.79 ~ 0.91	16.47 ~ 19.05	21
GX 340+0	197 ~ 565	535 ~ 840	0.55 ~ 0.83	17.97 ~ 27.18	22
GX 349+2	715	985	0.87	17.16	23
Sco X-1	532 ~ 902	842 ~ 1143	0.80 ~ 0.92	16.34 ~ 18.74	24
XTE J1701-462	502 ~ 651	761 ~ 945	0.82 ~ 0.87	17.33 ~ 18.34	25

Notes: The second and third columns show the frequency ranges of the lower- and upper-kHz QPOs. The fourth column shows the range of the inferred position parameter  $X(\equiv R/r$ , see equation (9)) based on AWOM. The fifth column shows the range of the emission radii of kHz QPOs.

†: The NS radii are assumed as 15 km.

References: 1. van Straaten et al. 2005, Wijnands et al. 2003; 2. Linares et al. 2005, Zhang et al. 2006b; 3. van Straaten et al. 2000, van Straaten et al. 2002, Boutelier et al. 2009; 4. van Straaten et al. 2003, Barret et al. 2005a, Jonker et al. 2000, Méndez et al. 1998; 5. Altamirano et al. 2008, Wijnands et al. 1997a, Bhattacharyya 2010, Di Salvo et al. 2003, Jonker et al. 2000, Jonker et al. 2002a, Lin et al. 2011; 6. Markwardt et al. 1999; 7. Ford et al. 1998a; 8. Di Salvo et al. 2001, van Straaten et al. 2002, Strohmayer et al. 1996, Migliari et al. 2003, Jonker et al. 2000, Méndez & van der Klis 1999a; 9. Wijnands et al. 1998c, Ford et al. 1998b; 10. Smale et al. 1997; 11. Boirin et al. 2000; 12. Barret et al. 2008; 13. Altamirano et al. 2010; 14. Wijnands & van der Klis 1997; 15. Kaaret et al. 2002; 16. Strohmayer et al. 2008; 17. Tomsick et al. 1999, Homan et al. 1999; 18. Boutloukos et al. 2006; 19. Wijnands et al. 1998a; 20. Wijnands et al. 1998b, Jonker et al. 2002b; 21. Homan et al. 2002, Wijnands et al. 1997b; 22. Jonker et al. 2002b, Wijnands et al. 1998a, Jonker et al. 1998; 23. O’Neill et al. 2002; 24. van der Klis et al. 1997, van der Klis et al. 1996, Lin et al. 2011, Méndez & van der Klis 2000; 25. Homan et al. 2007, Homan et al. 2010, Sanna et al. 2010.

predicts the following relations between the NS mass density, the emission position of the kHz QPOs and the twin kHz QPO frequencies:

$$\nu_1 = 629(\text{Hz})A^{-2/3}\nu_{2k}^{5/3}\sqrt{1 - \sqrt{1 - \left(\frac{\nu_{2k}}{1.85A}\right)^{2/3}}} \quad (5)$$

$$A = \sqrt{\frac{M}{M_\odot} \frac{1}{R_6^3}} \quad (6)$$

$$\rho = 4.75 \times 10^{14} A^2 (\text{g cm}^{-3}) \quad (7)$$

$$\nu_2 = \nu_1 X^{-5/4} \sqrt{1 + \sqrt{1 - X}} \quad (8)$$

$$X \equiv R/r \quad (9)$$

where  $\nu_{2k} = \nu_2/1000$  Hz,  $A$  is the parameter that is related to the NS mass density  $\rho$ ,  $M$  is the NS mass,  $R_6 = R/10^6$  cm is the NS radius  $R$  in unit of 10 km,  $X$  is the position parameter and  $r$  is the emission radius of the kHz QPOs refer

**Table 2.** The emission radii of kHz QPOs for the sources with measured NS masses<sup>‡</sup>.

Source (3)	Measured NS mass ( $M_{\odot}$ )	Ref	$A$ ( $\propto \rho^{1/2}$ )	$R$ (km)	$r$ (km)	$R_{\text{ISCO}}$ (km)
Cyg X-2	$1.71 \pm 0.21$	1	$0.62 \pm 0.04$	$16.4 \pm 1.02$	$21.23 \pm 1.60$	$15.12 \pm 1.86$
SAX J1808.4-3658	$< 1.4$	2	$0.43 \pm 0.01$	$18 \sim 20^{\parallel}$	$20 \sim 23^{\parallel}$	$9 \sim 12^{\parallel}$
XTE 1820-30	$1.29^{+0.19}_{-0.07}$	3	$0.65 \pm 0.01$	$14.5^{+0.7}_{-0.3}$	$16.2^{+0.8}_{-0.4} \sim 16.7^{+0.9}_{-0.4}$	$11.4^{+1.7}_{-0.6}$

Notes: The second column shows the measured NS masses. The fourth column shows the NS density parameter  $A$  ( $\equiv \sqrt{\frac{M}{M_{\odot}} \frac{1}{R_6^3}}$ , see equation (6)) inferred by the twin kHz QPO frequencies in Table 1. The fifth column shows the NS radii inferred by the measured NS masses and  $A$ . The sixth column shows the range of the emission radii of kHz QPOs inferred by the NS radii and position parameter  $X$  in Table 1. The last column shows the ISCO radii (i.e.  $R_{\text{ISCO}} = 3R_s = 6GM/c^2$ ).  
<sup>‡</sup>: See Table 1 for the twin kHz QPOs and position parameter  $X$ .

<sup>∥</sup>: The lower limit of the NS mass is adopted as  $1 M_{\odot}$  (see Miller 2002; Zhang et al. 2011).

Reference: 1. Casares et al. 2010; 2. Elebert et al. 2009; 3. Shaposhnikov & Titarchuk 2004.

to the center of the NS. According to AWOM, the NS mass density parameter  $A$  and the position parameter  $X$  can be inferred by the twin kHz QPO frequencies.

### 2.3 The sample of published kHz QPO frequencies

We search the literature for all published instances of kHz QPO frequencies, and constrain the sample to the detection of two simultaneous kHz QPO peaks. The sample includes 416 pairs of twin kHz QPOs from 25 NS-LMXB sources, where the 23 pairs are taken from the accreting millisecond X-Ray pulsars, and the 190/203 ones from Atoll/Z sources. The adopted sources with the ranges of the lower and upper kHz QPO frequencies and references are reported in Table 1. In addition, three sources in the sample have been measured with the NS masses, which are shown in Table 2.

## 3 THE EMISSION POSITIONS OF KHZ QPOS

We infer the emission radii of kHz QPOs based on AWOM. For the 22 sources without the measured NS masses (see Table 1), we take the following calculation steps:

- (1) For a certain pair of kHz QPO frequencies ( $\nu_1$  and  $\nu_2$ ), we first calculate the value of the position parameter  $X$  by solving equation (8):  

$$\nu_2 = \nu_1 X^{-5/4} \sqrt{1 + \sqrt{1 - X}}.$$
- (2) Then we infer the corresponding emission radius  $r$  of the kHz QPOs with the  $X$  value by equation (9):  $r = R/X$ , where the NS radius  $R$  is assumed to be 15 km.

While for the three sources with the measured NS masses (Cyg X-2, SAX J1808.4-3658 and XTE 1820-30, see Table 2), we first take the following steps to infer the NS radius  $R$  based on AWOM:

- (1) For each source, we fit the equation (5):  

$$\nu_1 = 629(\text{Hz}) A^{-2/3} \nu_{2k}^{5/3} \sqrt{1 - \sqrt{1 - \left(\frac{\nu_{2k}}{1.85A}\right)^{2/3}}}$$
to the twin kHz QPO frequencies and obtain the value of the NS density parameter  $A$ .
- (2) Then we infer the NS radius  $R$  of this source with the  $A$

value and the measured NS mass  $M$  by solving equation

$$(6): A = \sqrt{\frac{M}{M_{\odot}} \frac{1}{R_6^3}}.$$

Next we take the following steps to infer the emission radii of kHz QPOs for the three sources:

- (1) For a certain pair of kHz QPO frequencies, we calculate the  $X$  value with  $\nu_1$  and  $\nu_2$  by solving equation (8):  

$$\nu_2 = \nu_1 X^{-5/4} \sqrt{1 + \sqrt{1 - X}}.$$
- (2) Then we infer the corresponding emission radius  $r$  of the kHz QPOs with the  $X$  value and the inferred NS radius  $R$  by equation (9):  $r = R/X$ .

The ranges of the inferred  $X$  and  $r$  values for the sources without and with the measured NS masses are shown in Table 1 and Table 2, respectively. There are some aspects should be noticed:

- (1) The emission radii of kHz QPOs of AMXPs, Atoll and Z sources are distributed in the range of 18 – 31 km, 16 – 29 km and 16 – 38 km, respectively. Fig.1 shows the schematic diagram of the radial ranges of the emission positions of kHz QPOs for Atoll and Z sources. It is evidence that Z sources have the larger range of the emission radii of kHz QPOs than Atoll sources, which may result from source Cir X-1 with the large emission radii of 23.36 – 37.58 km (see also Fig.3).
- (2) We show the cumulative distribution function (CDF) curves of the position parameter  $X$  and the emission radius  $r$  of kHz QPOs for AMXPs ( $X = 0.49 - 0.88$ ,  $r = 18.18 - 30.51$  km), Atoll ( $X = 0.52 - 0.93$ ,  $r = 16.15 - 28.72$  km) and Z ( $X = 0.40 - 0.92$ ,  $r = 16.34 - 37.58$  km) sources in Fig.2. It can be seen that most of the emission radii of kHz QPOs of Atoll sources (> 90% of the data) and Z sources (> 70% of the data) cluster around the region of 16 – 19 km.
- (3) XTE J1807.4-294 ( $r = 18.18 - 30.51$  km), 4U 0614+09 ( $r = 17.02 - 28.72$  km), GX 5-1 ( $r = 16.90 - 29.69$  km) and GX 340+0 ( $r = 17.97 - 27.18$  km) show the larger range of the emission radii of kHz QPOs from  $\sim 17$  km to  $\sim 30$  km (see Table 1 for the details) than the other sources, and their corresponding CDF curves of the emission radii are shown in Fig.3.
- (4) We also analyze the innermost emission positions of kHz QPOs for all the sources in the sample. Fig.4 shows

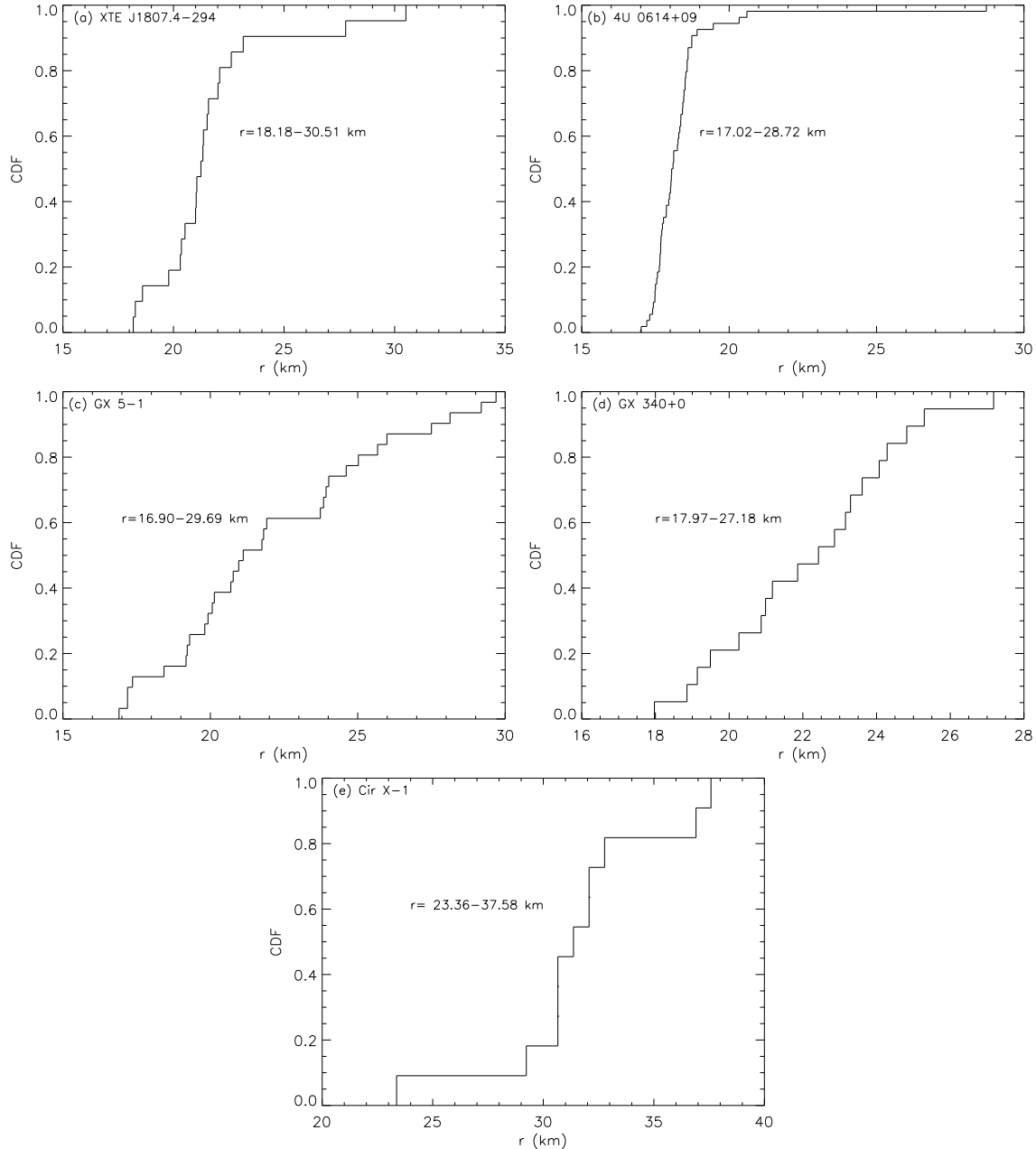


**Figure 3.** The CDF curves of the emission radii of kHz QPOs for (a) XTE J1807.4-294 ( $r = 18.18 - 30.51$  km), (b) 4U 0614+09 ( $r = 17.02 - 28.72$  km), (c) GX 5-1 ( $r = 16.90 - 29.69$  km), (d) GX 340+0 ( $r = 17.97 - 27.18$  km), (e) Cir X-1 ( $r = 23.36 - 37.58$  km), see Table 1 for the details.

the CDF curve of the minimal emission radii (16.15 – 23.36 km) of all the 25 sources, from which it can be seen that 22 sources share the minimal emission radii around the range of 16 – 19 km, while the other three sources, i.e. Cir X-1, Cyg X-2 and SAX J1808.4-3658, show the larger ones of about 23, 21 and 20 km, respectively.

#### 4 DISCUSSIONS AND CONCLUSIONS

We investigate the emission radii of kHz QPOs for the accreting millisecond X-ray pulsars, Atoll and Z sources based on AWOM, and find that most of the emission positions of

kHz QPOs cluster around the region of several kilometers away from the NS surface. The details of the conclusions are discussed and summarized as follows:

- (1) The inferred emission radii of kHz QPOs of AMXPs, Atoll and Z sources based on AWOM are distributed in the range of 18 – 31 km, 16 – 29 km and 16 – 38 km respectively (see Table 1, Table 2 and Fig.1 for the details). Cir X-1 has the obviously larger emission radii of 23.36 – 37.58 km than the other sources. It is thought that kHz QPOs reflect the motion of matter in orbit at some preferred radius  $r$  in the accretion disk (Miller et al. 1998; Stella & Vietri 1999;

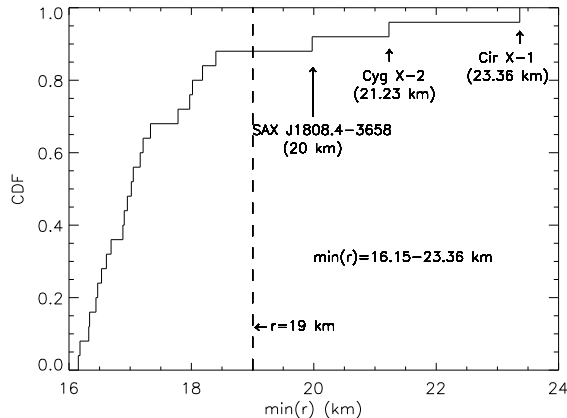


**Figure 4.** The CDF curve of the minimal emission radii of kHz QPOs (16.15–23.36 km) of all the 25 sources in Table 1 and Table 2. The dashed line shows the position of the emission radius of 19 km and the arrows indicate the innermost emission positions of source Cir X-1 ( $r_{\min} = 23.36$  km), Cyg X-2 ( $r_{\min} = 21.23$  km) and SAX J1808.4-3658 ( $r_{\min} = 20$  km) (see Table 1 and Table 2 for the details).

Osherovich & Titarchuk 1999; Lamb & Miller 2001; Zhang 2004), where the magnetosphere-disk radius there  $r_m = r$  satisfies the equation (3):

$$r_m \approx 7(\text{km}) \left( \frac{B_s}{10^{18} \text{ G}} \right)^{4/7} \left( \frac{\dot{M}}{10^{18} \text{ g s}^{-1}} \right)^{-2/7}.$$

We suggest that Cir X-1 may have the large NS surface magnetic field  $B_s$ , which will cause the large magnetosphere-disk radius, i.e. the large ones of the emission radii of kHz QPOs. It is not clear what physical parameters determine the appearance of the detectable kHz QPOs, nor why they only occur in the certain range of  $1 \sim \geq 20$  km away from the NS surface, and we suspect that it may be related to the accretion environment of LMXBs, which need the further study of the accretion state of the systems.

- (2) XTE J1807.4-294, 4U 0614+09, GX 5-1 and GX 340+0 show the larger range of the emission radii of kHz QPOs from  $\sim 17$  km to  $\sim 30$  km (see Table 1 and Fig.3), implying these sources may have the more suitable physical environment to produce kHz QPOs. Less bright source XTE J1807.4-294 ( $r = 18.18 \sim 30.51$  km) and 4U 0614+09 ( $r = 17.02 \sim 28.72$  km) have the similar large range of the emission radii with the more bright source GX 5-1 ( $r = 16.90 \sim 29.69$  km) and GX 340+0 ( $r = 17.97 \sim 27.18$  km), which implies the emission condition of kHz QPOs may not sensitive to the mean accretion rate.
- (3) It can be seen from see Table 1, Table 2 and Fig.2 that the emission radius  $r$  of kHz QPOs for all the sources are larger than the NS radius  $R$  ( $r > 16$  km and  $R$  is assumed to be 15 km, i.e.  $r > R$ ), which means that the accretion matter that is related to the kHz QPOs is at the position at least one kilometer away from the NS surface. There may be some interpretations for these phenomena: One is the effect of the local strong magnetic spot (Zhang et al. 2006a) which expels the magnetosphere-disk not to approach the NS surface, so the accretion matter may at the position away from the NS surface. Another explanation is that the accretion

plasma drops onto the stellar surface due to the instability when crossing the innermost stable circular orbit (ISCO) of NS, and the ISCO radius ( $R_{\text{ISCO}} = 6GM/c^2$ ) is the inner boundary of the accretion matter, so the emission radius of the kHz QPOs should be larger than  $R_{\text{ISCO}}$ . We try to test the ISCO effect scenario: Three sources in the sample, i.e. Cyg X-2, SAX J1808.4-3658 and XTE 1820-30, have both the detected twin kHz QPO frequencies and the measured NS masses (see Table 2), which can be used to calculate both the NS radii and ISCO radii with the following equations:

$$\nu_1 = 629(\text{Hz}) A^{-2/3} \nu_{2k}^{5/3} \sqrt{1 - \sqrt{1 - \left( \frac{\nu_{2k}}{1.85A} \right)^{2/3}}},$$

$$A = \sqrt{\frac{M}{M_\odot} \frac{1}{R_6^3}},$$

$$R_{\text{ISCO}} = 6GM/c^2.$$

The results are shown in Table 2, i.e. for Cyg X-2,  $R \sim 16.4$  km and  $R_{\text{ISCO}} \sim 15.12$  km, for SAX J1808.4-3658,  $R \sim 18 - 20$  km and  $R_{\text{ISCO}} \sim 9 - 12$  km, for XTE 1820-30,  $R \sim 14.5$  km and  $R_{\text{ISCO}} \sim 11.4$  km. It can be seen that the ISCO radii of the three sources are all smaller than their inferred NS radii, so we suggest that the ISCO effect may not be the main reason to cause the emission radii of the kHz QPOs larger than the NS radii.

- (4) It can be seen from Table 1, Table 2 and Fig.2 that most Atoll and Z sources (19/23) are inferred to share the similar emission radii of kHz QPOs of 16–19 km. We try to probe the NS magnetic field by the kHz QPOs: The luminosities of Atoll sources are less than those of Z sources in 2-3 magnitude orders in general, thus we assume that the accretion rates of Atoll sources are about 2 magnitude orders lower than those of Z sources in average. The magnetosphere-disk radius  $r_m$  where the kHz QPOs occur satisfy the equation (3):

$$r_m \approx 7(\text{km}) \left( \frac{B_s}{10^{18} \text{ G}} \right)^{4/7} \left( \frac{\dot{M}}{10^{18} \text{ g s}^{-1}} \right)^{-2/7},$$

the similar  $r_m (= 16 - 19$  km) and the different  $\dot{M}$  will infer the NS surface magnetic field strengths of Atoll sources are about one magnitude order less than those of Z sources, which is consistent with the prediction of Zhang et al. (2007). Source XTE J1701-462 has been observed both Atoll and Z behaviors (Homan et al. 2010), which can go from one state to the other one in timescale of months, and Homan et al. (2010) suggest this source has a NS surface magnetic field strength should not change in that timescale. We argue that XTE J1701-462 has a steady NS surface magnetic field and should not change in the short timescale, and ascribe the change of the Atoll and Z behaviors to the different magnetic field strengths at the different magnetosphere-disk radii: By assuming the NS magnetic field to be dipolar (see equation (2)):

$$B(r) = B_s \left( \frac{R}{r} \right)^3,$$

when the source has a instantaneously high accretion rate, the accretion disk will go closer to the NS surface and shows a smaller  $r_m$ , where the magnetic field there will be higher, then the source shows the Z source behavior. On the contract, the system will show the Atoll source behavior with the lower magnetic field at the magnetosphere-disk radius when it has a instantaneously low accretion rate. So we suggest that the Atoll

and Z states of the source may reflect the magnetic field information at the different magnetosphere-disk radii.

- (5) Cir X-1 ( $r_{\min} = 23.36$  km), Cyg X-2 ( $r_{\min} = 21.23$  km) and SAX J1808.4-3658 ( $r_{\min} = 20$  km) show the large values of the minimal emission radii of kHz QPOs compared with the other sources in the sample (see also Table 1, Table 2 and Fig.4). As for Cir X-1 and Cyg X-2, we try to ascribe their larger ones of the minimal emission radii to share the stronger NS surface magnetic fields that make the averaged magnetosphere-disk radii to be larger. For SAX J1808.4-3658, its inferred NS radius is slightly large ( $R = 18 - 20$  km with the NS mass of  $M = 1 - 1.4 M_{\odot}$ , see Table 2), so its emission radii of kHz QPOs are relative large although it has the similar emission parameter  $X$  values to the other sources ( $r = R/X$ ).

## ACKNOWLEDGMENTS

We thank J. Wang, Z.B. Li and H.X. Yin for helpful discussions. This work is supported by the National Basic Research Program of China (2012CB821800 and 2009CB824800), the National Natural Science Foundation of China NSFC(11173034, 11173024, 11303047), the Science and Technology Foundation of Guizhou Province (Grant No.J[2015]2113), the Doctoral Starting up Foundation of Guizhou Normal University 2014 and the Innovation Team Foundation of the Education Department of Guizhou Province under Grant Nos. [2014]35.

## REFERENCES

- Abramowicz M. A. et al., 2003a, *A&A*, 404, L21  
 Abramowicz M. A. et al., 2003b, *PASJ*, 55, 467  
 Altamirano D. et al., 2008, *ApJ*, 685, 436  
 Altamirano D. et al., 2010, *MNRAS*, 401, 223  
 Barret D. et al., 2005a, *MNRAS*, 357, 1288  
 Barret D. et al., 2005b, *MNRAS*, 361, 855  
 Barret D., Boutelier M., Miller M. C., 2008, *MNRAS*, 384, 1519  
 Belloni T., Psaltis D., van der Klis M., 2002, *ApJ*, 572, 392  
 Belloni T., Méndez M., Homan J., 2005, *A&A*, 437, 209  
 Belloni T., Méndez M., Homan J., 2007, *MNRAS*, 376, 1133  
 Bhattacharyya S., 2010, *Research in Astronomy and Astrophysics*, 10, 227  
 Boirin L. et al., 2000, *A&A*, 361, 121  
 Boutelier M., Barret D., Miller M. C., 2009, *MNRAS*, 399, 1901  
 Boutloukos S. et al., 2006, *ApJ*, 653, 1435  
 Casares J. et al., 2010, *MNRAS*, 401, 2517  
 Di Salvo T. et al., 2001, *ApJ*, 546, 1107  
 Di Salvo T., Méndez M., van der Klis M., 2003, *A&A*, 406, 177  
 Elebert P. et al., 2009, *MNRAS*, 395, 884  
 Ford E. C., van der Klis M., Kaaret P., 1998a, *ApJ*, 498, L41  
 Ford E. C. et al., 1998b, *ApJ*, 508, L155  
 Ford E. C., van der Klis M., 1998c, *ApJ*, 506, L39  
 Ford E. C. et al., 2000, *ApJ*, 537, 368  
 Ghosh P., Lamb F. K., 1979, *ApJ*, 234, 296  
 Hasinger G., van der Klis M. 1989, *A&A*, 225, 79  
 Homan J. et al., 1999, *ApJ*, 513, L119  
 Homan J. et al., 2002, *ApJ*, 568, 878  
 Homan J. et al., 2007, *ApJ*, 656, 420  
 Homan J. et al., 2010, *ApJ*, 719, 201  
 Jonker P. G. et al., 1998, *ApJ*, 499, L191  
 Jonker P. G., Méndez M., van der Klis M., 2000, *ApJ*, 540, L29  
 Jonker P. G., Méndez M., van der Klis M., 2002a, *MNRAS*, 336, L1  
 Jonker P. G. et al., 2002b, *MNRAS*, 333, 665  
 Kaaret P. et al., 1998, *ApJ*, 497, L93  
 Kaaret P. et al., 2002, *ApJ*, 575, 1018  
 Kluźniak W., Abramowicz M. A., 2001, *Acta Phys. Polonica B*, 32, 3605  
 Lamb F. K., Miller M. C., 2001, *ApJ*, 554, 1210  
 Lin Y. F. et al., 2011, *ApJ*, 726, 74  
 Linares M. et al., 2005, *ApJ*, 634, 1250  
 Markwardt C. B., Strohmayer T. E., Swank, J. H., 1999, *ApJ*, 512, L125  
 Mauche C. W., 2002, *ApJ*, 580, 423  
 Méndez M. et al., 1998, *ApJ*, 505, L23  
 Méndez M., van der Klis M., 1999a, *ApJ*, 517, L51  
 Méndez M. et al., 1999b, *ApJ*, 511, L49  
 Méndez M., van der Klis M., 2000, *MNRAS*, 318, 938  
 Méndez M., van der Klis M., E. C. Ford, 2001, *MNRAS*, 561, 1016  
 Méndez M., 2006, *MNRAS*, 371, 1925  
 Migliari S., van der Klis M., Fender R. P., 2003 *MNRAS*, 345, L35  
 Miller M. C., Lamb F. K., Psaltis D., 1998, *ApJ*, 508, 791  
 Miller M. C., 2002, *Nat*, 420, 31  
 O'Neill P. M. et al., 2002, *MNRAS*, 336, 217  
 Osheroich V., & Titarchuk L., 1999, *ApJ*, 522, L113  
 Psaltis D., Belloni T., & van der Klis M. 1999, *ApJ*, 520, 262  
 Sanna A. et al., 2010, *MNRAS*, 408, 622  
 Shapiro S. L., Teukolsky S. A., 1983, *Black Holes, White Dwarfs, and Neutron Stars: The Physics of Compact Objects*. Wiley Interscience, New York  
 Shaposhnikov N., Titarchuk L., 2004, *ApJ*, 606, L57  
 Smale A. P., Zhang W., White N. E., 1997, *ApJ*, 483, L119  
 Stella L., Vietri M., 1999, *Phys. Rev. Lett.*, 82, 17  
 Stella L., Vietri M., Morsink S. M., 1999, *ApJ*, 524, L63  
 Strohmayer T. E. et al., 1996, *ApJ*, 469, L9  
 Strohmayer T. E., Markwardt C. B., Swank J. H., 2008, *Astron. Telegram*, 1635, 1  
 Stuchlík Z., Kotrlová A., Török G., 2013, *A&A*, 522, A10  
 Tomsick J. A. et al., 1999, *ApJ*, 521, 341  
 van der Klis M. et al. 1996, *ApJ*, 469, L1  
 van der Klis M. et al. 1997, *ApJ*, 481, L97  
 van der Klis M., 2000, *ARA&A*, 38, 717  
 van der Klis M., 2001, *ApJ*, 561, 943  
 van der Klis M., 2006, in Lewin W. H. G., van der Klis M., eds, *Compact Stellar X-Ray Sources*, Cambridge Univ. Press, Cambridge, p.39  
 van Straaten S. et al., 2000, *ApJ*, 540, 1049  
 van Straaten S. et al., 2002, *ApJ*, 568, 912  
 van Straaten S., van der Klis M., Méndez M., 2003, *ApJ*, 596, 1155  
 van Straaten S., van der Klis M., Wijnands R., 2005, *ApJ*, 619, 455

- Wang D.H. et al., 2013, MNRAS, 435, 3494  
Wang D.H. et al., 2014, Astron. Nachr., 335, 168  
Warner B., & Woudt P. A., 2002, in ASP Conf. Ser. 261,  
The Physics of Cataclysmic Variables and Related Object,  
ed. B. T. Gänsicke, K. Beuermann, & K. Reinsch (San  
Francisco: ASP), 406  
Wijnands R. et al., 1997a, ApJ, 479, L141  
Wijnands R. et al., 1997b, ApJ, 490, L157  
Wijnands R., van der Klis M., 1997, ApJ, 482, L65  
Wijnands R. et al., 1998a, ApJ, 493, L87  
Wijnands R. et al., 1998b, ApJ, 504, L35  
Wijnands R. et al., 1998c, ApJ, 495, L39  
Wijnands R. et al., 2003, Nat, 424, 44  
Zhang C. M., 2004, A&A, 423, 401  
Zhang C. M. et al., 2006a, MNRAS, 366, 1373  
Zhang C. M., et al., 2007, Astron. Nachr., 328, 491  
Zhang C. M. et al., 2011, A&A, 527, 83  
Zhang F. et al., 2006b, ApJ, 646, 1116

This paper has been typeset from a  $\text{\TeX}$ / $\text{\LaTeX}$  file prepared  
by the author.